Journal of Nuclear Materials 403 (2010) 152–159

Contents lists available at ScienceDirect

Journal of Nuclear Materials

journal homepage: www.elsevier.com/locate/jnucmat

Development of silicide coating over molybdenum based refractory alloy and its characterization

S.P. Chakraborty [*], S. Banerjee, I.G. Sharma, A.K. Suri

Materials Processing Division, Bhabha Atomic Research Center, Trombay, Mumbai 400 085, India

ARTICLE INFO

Article history:
Received 26 October 2008
Accepted 7 June 2010

ABSTRACT

Molybdenum based refractory alloys are potential candidate materials for structural applications in high temperature compact nuclear reactors and fusion reactors. However, these alloys being highly susceptible to oxidation in air or oxygen at elevated temperature, undergoes severe losses from highly volatile molybdenum trioxide species. Present investigation, therefore, examines the feasibility of development of silicide type of coating over molybdenum base TZM alloy shape (Mo > 99 wt.%) using pack cementation coating technique. TZM alloy was synthesized in this laboratory from oxide intermediates of MoO_2, TiO_2 and ZrO_2 in presence of requisite amount of carbon, by alumino-thermic reduction smelting technique. The arc melted and homogenized samples of TZM alloy substrate was then embedded in the chosen and intimately mixed pack composition consisting of inert matrix (Al_2O_3), coating powder (Si) and activator (NH_4Cl) taken in the judicious proportion. The sealed charge packs contained in an alumina crucible were heated at temperatures of 1000 °C for 8–16 h heating cycle to develop the coating. The coating phase was confirmed to be of made of $MoSi_2$ by XRD analysis. The morphology of the coating was studied by SEM characterization. It had revealed that the coating was diffusion bonded where Si from coating diffused inward and Mo from TZM substrate diffused outward to form the coating. The coating was found to be resistant to oxidation when tested in air up to 1200 °C. A maximum 100 μm of coating thickness was achieved on each side of the substrate.

1. Introduction

Molybdenum base refractory alloys are potential candidate materials for new generation high temperature compact nuclear and fusion reactors. Amongst the various molybdenum rich alloys, TZM alloy (Mo > 99%) is one of the most promising one. The alloy offers several attributes for high temperature structural applications including high melting temperature (>2600 °C), high creep strength at elevated temperature, good corrosion compatibility with many molten metal and alloys, specially molten Zn, Pb and Pb–Bi eutectic between 800 and 1000 °C. However, these alloys are highly susceptible to oxidation when subjected to hot working in oxidizing environment. The oxidation takes place due to formation of non protective and volatile oxides on the metal or alloy surface at intermediate temperature zone which subsequently evaporate at higher temperature at a slow or rapid rate depending upon the oxidation kinetics of the surrounding environment. In consequence, the refractory metal or alloy loses its material integrity resulting in loss of several vital properties. In TZM alloy, molybdenum being the major element present along with minor components such as Ti, Zr and C, plays a crucial role in influencing the oxidation behaviour of TZM alloy. Studies of molybdenum at high level of oxygen as conducted by investigators indicated that molybdenum on oxidation between 450 °C and 650 °C forms MoO_2 and other sub-oxides (MoO_z) where $2 < Z < 3$ and MoO_3 above 650 °C. The rate of oxidation for pure molybdenum between 250 and 450 °C follows a parabolic pattern, above 400 °C, a linear pattern and above 650 °C, high vaporization of MoO_3 with mass loss and rapid oxidation rates. Many of the studies oriented toward extremely high temperatures e.g., up to 1700 °C, often under environments with low activities of oxygen had also shown considerable rate of oxidation of TZM alloy [1].

Alloying and coating are two techniques applied to provide protection for metals and alloys from oxidation. In case of alloying, the metal substrate is alloyed with another metal that prevents the oxidation of the parent metal by forming a thin passive layer of oxide. However, this type of coating does not offer any effective barrier to oxygen at high temperature. Therefore, in this context, surface coating of refractory metals and alloys become essential, prior to their use in high temperature oxidizing areas. A considerable research efforts have been made in the recent past on the development of silicide type of protective coating over various alloy substrates mostly on nickel based super alloys and Nb based refractory alloys by pack cementation technique because of their

---

[*] Corresponding author. Tel.: +91 22 25593931; fax: +91 22 25505151/25519613.
E-mail address: spc@barc.gov.in (S.P. Chakraborty).

0022-3115/$ - see front matter © 2010 Elsevier B.V. All rights reserved.
doi:10.1016/j.jnucmat.2010.06.014

extensive applications in various fields. Despite the well-known fact that the presence of aluminide and silicide type of coatings over molybdenum based alloys drastically improves their oxidation properties, however very few studies have been systematically carried out to develop the above coatings in such alloy system. In this context, it is worthwhile to mention here the detailed study carried out by investigators in understanding the mechanism of pack cementation technique and the effects of pack composition and time on the feasibility of forming aluminide coating on a nickel based super alloy by pack cementation technique [2]. In the subsequent study, aluminide coating was developed over TZM alloy in this laboratory using chloride halide pack by pack cementation technique [3]. In a recent publication, Majumdar et al. had evaluated the formation of $MoSi_2$ coating over TZM alloy using a fluoride halide pack at temperature of 1200 °C. Further, the study concluded that apart from $MoSi_2$ coating, a thin layer of Mo_5Si_2 was also formed over TZM alloy. Recently, mixed chloride and fluoride pack was explored to develop oxidation resistant silicide and Al–Si composite coatings over Mo–30W alloy [4]. In another piece of work, the formative mechanism of $MoSi_2$ coating over Mo precoated Nb based alloy C103 was studied [5].

A number of coating techniques are available for providing surface protection, namely, physical vapour deposition (PVD), chemical vapour deposition (CVD), pack cementation, thermal spray coating, vacuum plasma coating, laser surface alloying, etc. Although, many of these techniques are employed in various capacities in industrial practice, however, they are not devoid of any flaws and have several limitations. PVD technique provides reasonably good coating but the coating thickness obtained is very thin (5–10 μm) that usually have poor mechanical bond. This technique further requires atmosphere of vacuum for coating and as a result, coating of any intricate parts becomes relatively difficult. CVD technique, on the other hand, is employed for only limited number of coatings and the technique becomes increasingly difficult for composite and ceramic coatings using reactive pack. Plasma assisted chemical vapour deposition (PACVD) technique employs coating guided by plasma. However, this kind of coating provides a porous surface due to low deposition rate. Halide activated pack cementation (HAPC) technique on the other hand, is basically a kind of in situ chemical vapour deposition technique where the metal halide vapours formed due to chemical reactions of the corresponding packing materials get reduced on the surface of the substrate to develop a protective layer of the desired metal coating. Since this is basically a diffusion controlled process, the metallurgical bond that forms between the substrate and the coating is excellent. This technique has several advantages over others. It is easy to operate, inexpensive, can accommodate samples of varying size and shape and above all, can provide uniform and smooth coating of desired thickness. However, there is no meaningful literature or published reports available on the application of such techniques to provide oxidation resistant coating on TZM alloys. Transition metal silicides have many attractive properties such as high melting point, relatively low density, high stiffness as well as excellent oxidation and creep resistance, and are recognized as promising candidate for high temperature structural materials. The strong atomic bond and ordered crystal structure also provide the material high strength, high elastic modulus and anomalous hardness-temperature dependence. These unique properties are visible prominently in $MoSi_2$, Cr_3Si, Ti_5Si_3 and $MoSi_2$-based composites [6].

Hence, in the present investigation, attempts were made to develop protective coating of molybdenum di-silicide over TZM alloy using pack cementation coating technique. The formation of the protective layer was rapid enough to suppress the damage due to the volatile oxide, MoO_3. During the coating process, active silicon was formed over the TZM alloy surface, which later on diffused into the substrate forming molybdenum di-silicide. The morphology and characteristics of the coating were studied by a combination of SEM, Optical and XRD analysis and the physical properties of the coating were evaluated with respect to hardness, oxidation, etc.

2. Experimental

2.1. Materials

2.1.1. Substrate

TZM alloy, experimentally prepared in this laboratory was selected as a substrate for coating. The alloy was initially synthesized from the oxide intermediates of Mo, Ti and Zr by alumino-thermic co-reduction technique in presence of requisite amount of carbon. Thermal energy of the chemical reactions involved during smelting was utilized to synthesize the TZM alloy. As-synthesized alloy button was later on melt consolidated by double arc argon melting. The consolidated button was subsequently heated to 1000 °C in vacuum and held at this temperature for 12 h for homogenization. The chemical composition of standard TZM alloy and experimentally synthesized alloy was presented in Table 1. Finally the buttons were sliced into of dimension 20 mm × 10 × 3 mm (l × b × h) by low speed diamond cutter. The corner and edges of the specimen were rounded off using abrasive grinding wheel. After smoothening, the specimens were polished using emery papers to remove any oxide layers and to obtain scratch free surface. Then the specimens were kept for cleaning in ultrasonic cleaner for 15–20 min to remove any dirt or grease from the surface of the specimen. The weight and dimension of the cleaned specimen were measured using electronic balance and eddy current tester.

Coating material: High pure silicon powder having -325 mesh particle size.
Activator: Ammonium chloride (LR grade).
Inert filler: Alumina (LR grade).
Cementing material: High temperature setting cement (TRIMOR).

A homogeneous pack mixture was prepared taking 43.5 g of dried alumina powder (filler), 3.5 g of silicon powder (coating substance), 3 g of ammonium chloride (activator). Alumina crucible having 35 mm id and 50 mm height was used to conduct the pack cementation experiments. The intimately mixed charge was poured inside the alumina crucible and tightly packed to ensure complete removal of air. Subsequently the specimens were embedded inside the pack horizontally, equidistant to each other in the crucible. The crucible was closed with alumina lid and sealed with high temperature setting cement. The sealed crucible was dried at RT overnight and then thoroughly cured at different intermediate temperatures of 70 °C, 150 °C and 300 °C for a total period of 5 h. The pack was then loaded inside a horizontal rectangular furnace. The furnace was flushed with argon gas to drive out residual air inside the furnace. Then the temperature of the furnace was raised to

Table 1
Composition of standard and experimentally synthesized TZM specimens.

Elements	Ti	Zr	C	Mo
TZM alloy Standard composition (wt.%)	0.5	0.08	0.02	Bal.
TZM alloy Experimental composition (wt.%)	0.45	0.1	0.06	Bal.

300 °C and held for 3 h in order to facilitate further curing of the cement and remove any moisture present in the pack. After this final curing, the temperature was gradually increased at a heating rate of 3–4 °C/min and the sealed crucible was annealed at 1000 °C for 8 h, 12 h and 16 h under argon atmosphere. On completion of the experiment, the furnace was air cooled and the pack was removed from the furnace at RT. Subsequently the specimens were recovered by opening the pack. Then the specimens were first cleaned under the jet of water to remove loosely attached pack charge particles. Later, these specimens were ultra-sonically cleaned and then dried. The weight and dimension of the specimens were measured and simultaneously weight gain per unit area of the specimen was calculated. Thickness of the specimens was measured by Eddy current tester.

2.2. Characterization and property evaluation studies

The elemental compositions of as-synthesized TZM alloy and standard TZM alloy were analyzed using standard gravimetric–volumetric techniques coupled with XRF analytical technique.

The microstructure of TZM alloys and corresponding coating were studied by optical microscopy. The TZM alloy specimens and transverse cut coated specimen were mounted in an epoxy resin and then polished by successive grades of emery papers (80–600 grit size) and finally by diamond polishing to obtain mirror finish specimens. The polished specimens were then suitably etched using a chemical etchant composed of hydrofluoric acid, nitric acid and lactic acid taken in the ratio 1:2:6 by volume. The microstructure of the etched specimen was revealed by an optical microscope at a magnification of 100–200×.

X-ray diffraction technique was employed to identify the various phases and species present in the alloy and corresponding coating species using Cu Kα radiation (wavelength = 0.154 nm) with a nickel filter and a secondary beam monochromator. The coated surface was scanned from 10° to 70° with a scanning rate of 2°/min.

The surface characteristics and coating morphology were studied by a TESCAN Vega make MV 2300T model Scanning electron microscope under a magnification of 1–1.5 kX. The elemental analysis of the coating was performed by the accompanying EDS system.

The hardness on the transverse and longitudinally cut surfaces of the coated and uncoated specimen was measured by a Microhardness tester at different locations using a load of 50 g for 10 s duration.

The oxidation behaviour of uncoated TZM alloys was evaluated by heating them isothermally from 200 °C to 1000 °C for a heating cycle of 1–6 h in air. Similarly, the coated TZM alloy specimens were heated isothermally at 1000 °C and 1200 °C for a 10–50 h heating cycle in air to evaluate the resistance to oxidation. The initial and final weight of the specimens before and after heating was recorded.

3. Results and discussion

3.1. Thermodynamic consideration and mechanism of coating

In the pack cementation process, the chemical reactions that are likely to take place are hereby expressed by following set of chemical equations

In the charge:

$$NH_4Cl(S) = NH_3(g) + HCl(g) \tag{i}$$

$$2NH_3(g) = N_2(g) + 3H_2(g) \tag{ii}$$

$$4HCl(g) + Si(l) = SiCl_4(g) + 4H \tag{iii}$$

On the substrate:

$$3SiCl_4(g) + Si(s) = 4SiCl_3(g) \tag{iv}$$

$$2SiCl_3(g) + Si(s) = 3SiCl_2(g) \tag{v}$$

$$SiCl_2(g) + Si(s) = 2SiCl(g) \tag{vi}$$

$$H(g) + Cl(g) = HCl(g) \tag{vii}$$

$$Si + Cl_2 + H_2 = SiH_2Cl_2 \tag{viii}$$

$$Si + (3/2)Cl_2 + 1/2(H_2) = SiHCl_3 \tag{ix}$$

$$Mo + 2Si = MoSi_2 \tag{x}$$

During the pack cementation process, the halide activator, namely, NH_4Cl initially dissociated into NH_3 and HCl vapours at a temperature higher than 350 °C as per the reaction (i). As the temperature increased further, the partial pressure of both the gases increased proportionately resulting in the formation of N_2 and H_2 gases as per reaction (ii). The HCl vapour further reacted with Si powder as per the reaction (iii) to form the volatile species, $SiCl_4$. Subsequently, three other lower chlorides, such as $SiCl_3$, $SiCl_2$ and SiCl were formed in quick succession from $SiCl_4$ by the reaction with Si. Apart from these volatile species, other two chlorides such as SiH_2Cl_2 and $SiHCl_3$ were formed from Si with the reaction of H_2 and Cl_2. Finally, H_2 and Cl_2 combined together to form HCl gas. The HCl vapour, meanwhile, etched the substrate surface helping the easy diffusion of Si into the sub-surface region and thus resulted in the synthesis of a $MoSi_2$ coating layer by the metallurgical reaction as per Eq. (x). The HCl gas was finally transferred back to the matrix where it again reacted with the released Cl (g) while the gaseous species deposited Si on substrate. This way the cycle of formation of volatile chloride species and deposition of Si over the TZM alloy substrate through the process of dissociation continued uninterrupted as long as the favourable conditions of reaction temperature and time were available [7].

The feasibility of formation of the gaseous species namely, SiCl, $SiCl_2$, $SiCl_3$, $SiCl_4$, $SiHCl_2$ and $SiHCl_3$ during cementation process was verified by evaluating the equilibrium partial pressure of each component. In this regard, first the equilibrium constant (k_p) for each reaction was calculated using the thermochemical data from JANAF table. The calculated values of equilibrium constant (k_p) of

Table 2
Results of coating experiments.

Coating samples	Weight gain (g)	Thickness (μm)	Time of run (hrs)	Remarks
1	0.0127	20	8	Coating inhomogeneous
2	0.0138	30		
3	0.0156	50		
4	0.0247	90	12	Coating homogeneous, adherent, non-porous
5	0.0281	100		
6	0.031	110		
7	0.0905	210	16	Coating homogeneous on surface but inhomogeneous at edges
8	0.0924	200		
9	0.0902	180		

Table 3
Calculated equilibrium partial pressures of different chlorides at 1000 °C.

Species present in gas phase	Calculated equilibrium partial pressure (atm)
$SiCl_4$	2.16×10^{-9}
$SiCl_3$	3.21×10^{-8}
$SiCl_2$	2.83×10^{-6}
SiCl	2.35×10^{-10}
SiH_2Cl_2	1.96×10^{-7}
$SiHCl_3$	2.54×10^{-8}

Table 4
Logarithms of the equilibrium constants of various reactant gas species formed in the Si–Cl–H system at 1000 °C.

Species	Log(K) (1000 °C)
$SiCl_4$	20.385
$SiCl_3$	14.201
$SiCl_2$	26.22
SiCl	−2.692
SiH_2Cl_2	8.305
$SiHCl_3$	14.775

various reactant gas species formed in the Si–Cl–H system at 1000 °C was presented in Table 3. Considering total pressure inside the pack as one atmosphere and using mass balance approach, the equilibrium partial pressure of components such as SiCl, $SiCl_2$, $SiCl_3$, $SiCl_4$, $SiHCl_2$, $SiHCl_3$ in a pack mixture consisting of 7 wt.% Si, 6 wt.% NH_4 Cl, and 87 wt.% Al_2O_3 have been calculated. $MOCl_x$ components cannot be formed at 1000 °C due to thermodynamic instability. Finally, the number of equations obtained was equal to the number of unknowns that are partial pressure of different gaseous species present in the pack [8]. The calculated equilibrium partial pressures of all the chlorides at 1000 °C are presented in Table 4. In this silicon pack cementation process, as per the equilibrium partial pressure data as presented in Table 4, all the chlorides of SiCl, $SiCl_2$, $SiCl_3$, $SiCl_4$, $SiHCl_2$, $SiHCl_3$ have registered high equilibrium partial pressures values at the processing temperature and therefore, are collectively responsible for the deposition of Si on the surface of substrate for coating as per the above chemical reactions. However, $SiCl_2$ and $SiHCl_2$ have recorded higher equilibrium partial pressures (2.83×10^{-6} atm and 1.96×10^{-7} atm) at 1000 °C as compared to other volatile phases. Hence, these species play dominant role in the deposition of Si on the surface of the substrate. $SiCl_4$ although has registered high vapour pressure value (2.16×10^{-9}) but it is not thermodynamically as stable as other phases at 1000 °C [9,10].

A number of pack cementation experiments were conducted by varying the principal variants Si and NH_4Cl concentration from 1 wt.% to 15 wt.% in the original packs to optimize the composition of pack and to study their effects on the structure of coating and its thickness. The optimized pack composition corresponded to 87 wt.% inert Al_2O_3, 7 wt.% Si and 6 wt.% NH_4Cl. As the concentration of Si and NH_4Cl were increased in the pack, the partial pressure of $SiCl_4$ increased proportionately. This led to the acceleration of coating process. Coating thickness also correspondingly increased. However, when the concentration of Si in the pack reached beyond 7 wt.% and that of NH_4Cl beyond 6 wt.%, the Si deposition rate became much faster resulting in rampant and non uniform growth of coating over the TZM substrate. The thickness of the coating correspondingly increased unceasingly with time. Coating was found to be brittle at the edges due to overgrowth. Finally when the concentration of Si and NH_4Cl in the pack were enhanced beyond 10 wt.%, the pressure inside the pack container was unusually large due to accumulation of chloride vapours leading to the opening of the pack lid with the release of gases.

The results of the various coating experiments performed at 8–16 h heating period at temperature of 1000 °C using pack cementation technique were summarized in Table 2. The experiments were carried out under similar experimental conditions for three times to substantiate the results. It was noticeable that the silicide coating thickness was enhanced remarkably with increase in holding time and the coating was homogeneously formed all over the substrate including the corners and edges with longer duration. However, slight coating overgrowth was observed at the edges of the specimens after 16 h of holding. The overall coating thickness varied from 200 to 210 μm including both sides. An optimum coating thickness of 100 μm on each side of the sample with corresponding weight gain 2.41 mg/cm^2 was obtained under the optimum experimental conditions at the temperature at 1000 °C for 12 h heating.

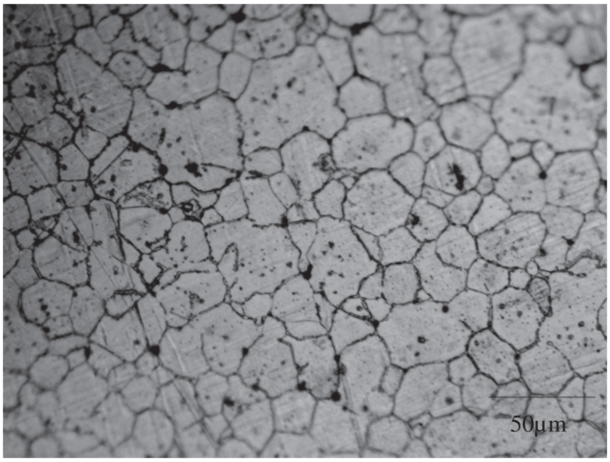

Fig. 1. Optical micrograph of experimentally synthesized TZM alloy.

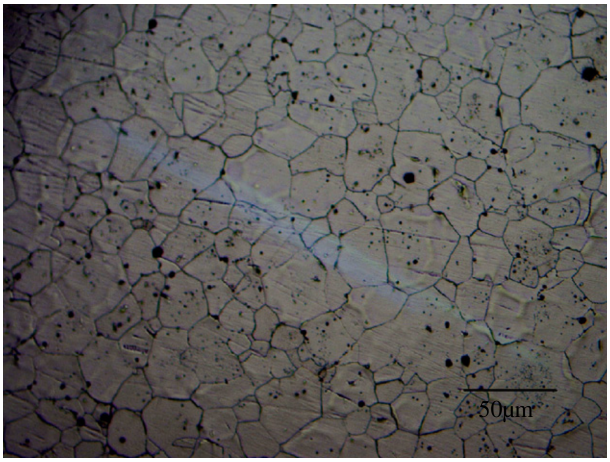

Fig. 2. Optical micrograph of standard TZM alloy.

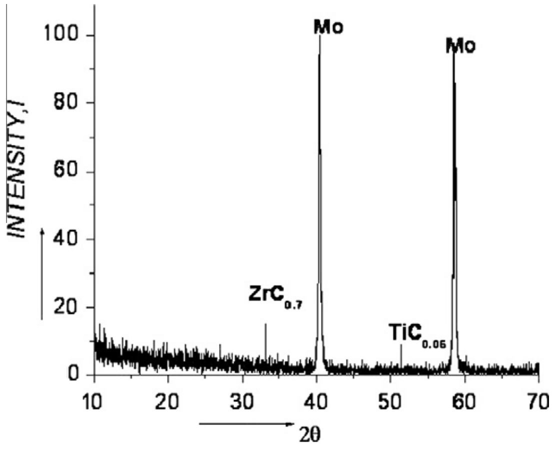

Fig. 3. X-ray diffraction pattern of synthesized TZM alloy.

One basic problem arises in $MoSi_2$ based coating on Mo is the mismatch strains generated between the coating layer and substrate due to the difference between the thermal expansion coefficients of $MoSi_2$ ($8.56 \times 10^{-6}\,°C^{-1}$) and molybdenum ($5.6 \times 10^{-6}\,°C^{-1}$) . During deposition at temperatures in the range 1000–1050 °C, the coating and substrate remain unstressed, however, during the stage of cooling, tensile stresses are created since $MoSi_2$ contracts more than the molybdenum substrate. These stresses are large enough to develop cracks since $MoSi_2$ has a negligible ductility below 800 °C. Although the cracks may heal by reheating at a lower application temperature than the range of 650–1000 °C or suitable oxide formation is required for self-healing [11].

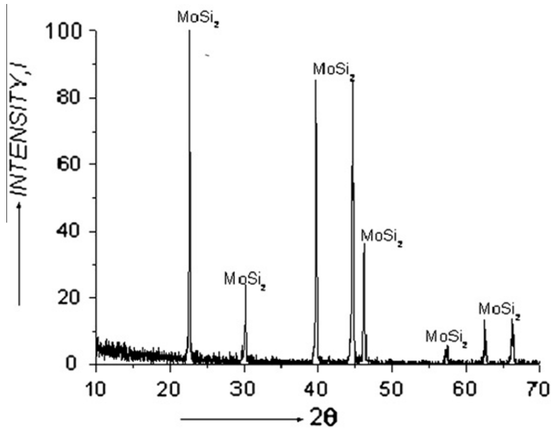

Fig. 4. X-ray diffraction pattern of silicide coating over TZM substrate.

In TZM alloy, the minor alloying elements of Ti and Zr are known to enhance oxide formation. The alloy containing these small additions of Ti and Zr, undergoes internal oxidation at temperature above 1000 °C with the formation of titanium and zirconium oxides. These oxides are conducive in sealing any cracks developed in $MoSi_2$ coating. There lies the effectiveness of using TZM substrate over Mo although these materials have no significant difference in molybdenum content. So, in case of TZM alloy, premature failure by oxidation can be avoided by oxide formation.

3.2. Results on characterization studies

3.2.1. Microstructural study

The optical micrograph of laboratory synthesized and standard TZM alloys, were presented in Figs. 1 and 2. The first alloy was subsequently used as a substrate for coating. The micrograph at Fig. 1 exhibited a granular structure with a combination of fine, intermediate and coarse grains in the form of round to hexagonal shapes with definite grain boundaries. The grain size varied from 10 to 75 μm. The nodular shaped carbides of zirconium and titanium were distributed along the grain boundaries and the matrix. The micrograph of laboratory prepared TZM alloy was matching with the micrograph of standard TZM alloy.

3.2.2. Identification of phases by X-ray diffraction

The X-ray diffraction (XRD) patterns of the substrate (TZM alloy) and that of coating on TZM alloy were presented in Figs. 3 and 4 respectively. The major intensity peaks in Fig. 3

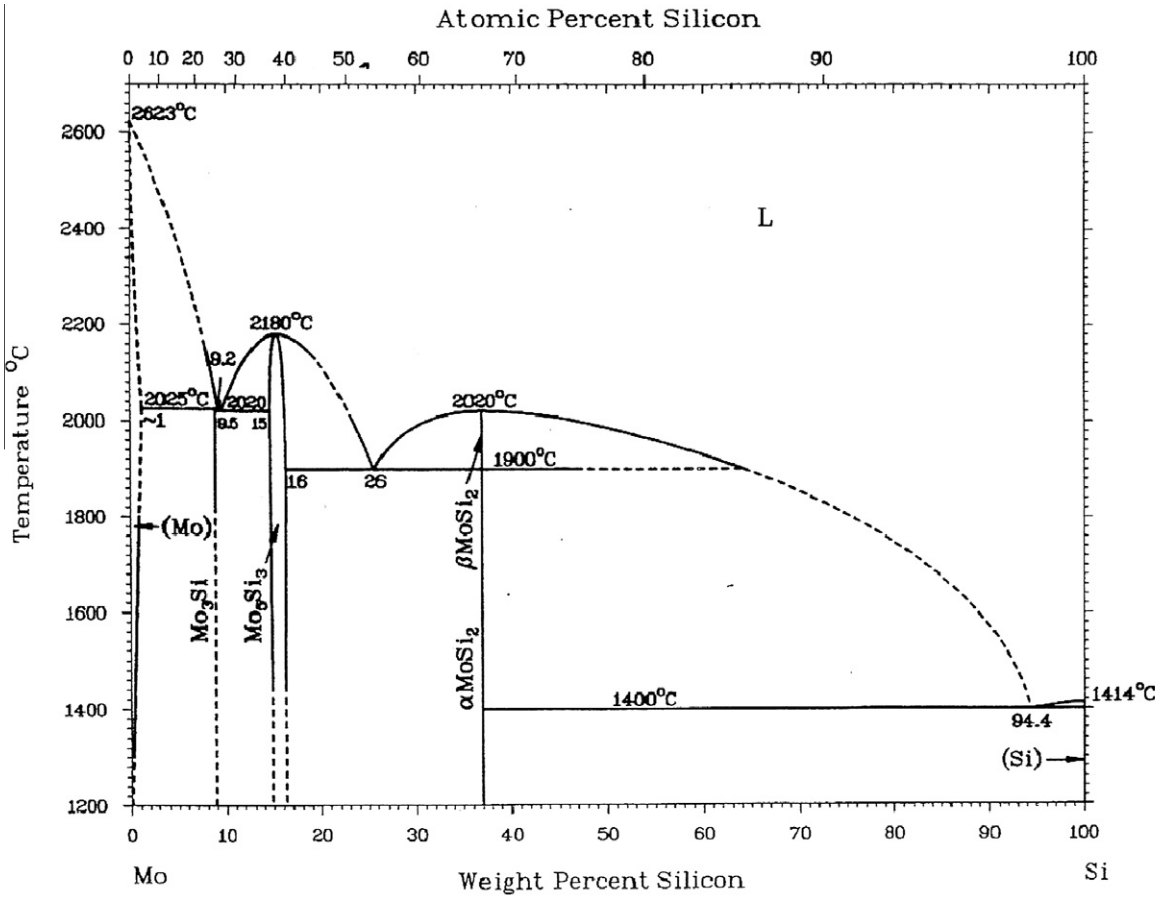

Fig. 5. Binary phase diagram of Mo–Si system.

corresponded to elemental Mo and the minor peaks to carbides of Ti and Zr. The intensity peaks in Fig. 4 corresponded to the phases of molybdenum di-silicides ($MoSi_2$). However, diffraction peaks of either elemental Mo or Si were not identified. XRD study, thus identified $MoSi_2$ as the reaction product of the silicide layer formed over TZM alloy surface. The formation of $MoSi_2$ type di-silicide phase was also predicted in the binary phase diagram of Mo–Si system at Fig. 5 at a composition of 35 wt.% Si and 65% Mo. The XRD at the cross section further confirmed the formation of Mo_5Si_3 along with $MoSi_2$ layer. There are three silicide phases, Mo_3Si, Mo_5Si_3 and $MoSi_2$, identified on the Mo–Si binary equilibrium phase diagram as indicated in Fig. 5. Tortorici et al. after a detailed investigation on the Mo–Si diffusion couple reported that the Mo_3Si layer could not form below 1350 °C due to nucleation difficulties. The thickness of the Mo_5Si_3 layer formed near Mo surface was very small. The growth rate of the $MoSi_2$ was much faster than that of Mo_5Si_3 in the temperature range of 900–1350 °C [12]. Present results are consistent with the above observations.

3.2.3. Surface morphology and interfacial study by SEM

The surface morphology of silicide coating on TZM alloy was depicted by SEM micrographs at magnifications of 1 kX, 10 kX and 25 kX in Figs. 6–8 respectively. The formation of a dense surface coating over the TZM alloy substrate was revealed by the micrograph at Fig. 6. The coating particles of different sizes got intermingled with each other to form clusters which provided good interlocking of coating material leading to adequate strength against peeling off. The coating was also homogeneously distributed and randomly oriented. There were abundant phase-interfaces in the coating. These phase-interfaces could play an important role of baffling the enlarging of the cracks by relaxing the stress at the top end of the cracks in the coating and inducing crack deflection, which was advantageous in avoiding the formation of through-coating cracks and improving the oxidation protective ability of the coating. It was distinctly shown in Fig. 7 that the smaller coating particles were adhered on the surface of larger particles. The interlocking of coating particles was clearly depicted at Fig. 8 at a comparatively higher magnification. The SEM image of the interfacial region between coating and TZM substrate at Fig. 9 had distinctly shown the distinguishing line between the coating and the substrate. A double layer coating structure was formed over TZM substrate. The inner coating layer adjacent to

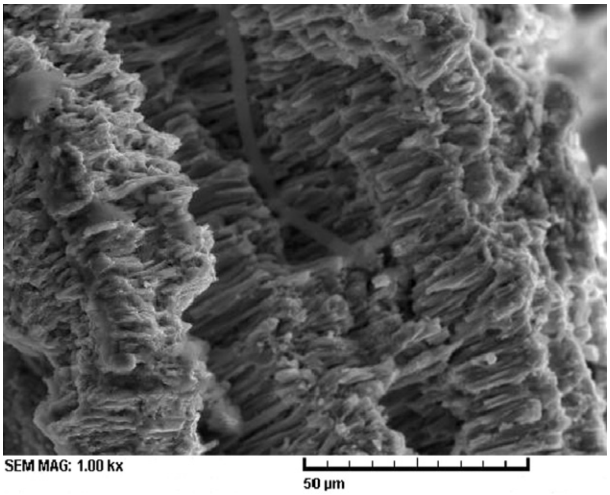

Fig. 6. SEM micrograph of silicide coating at low magnification.

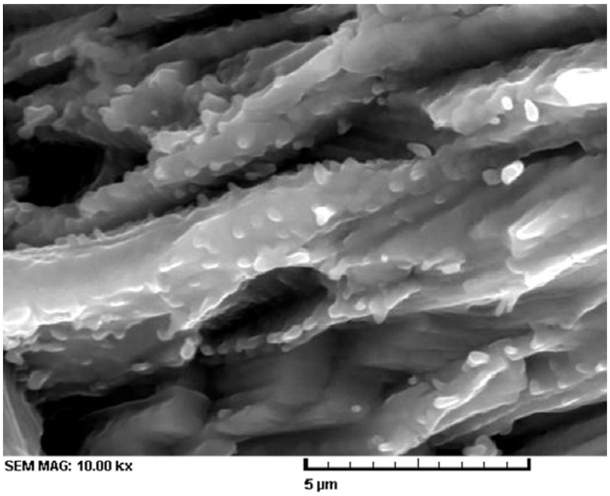

Fig. 7. SEM micrograph of silicide coating at medium magnification.

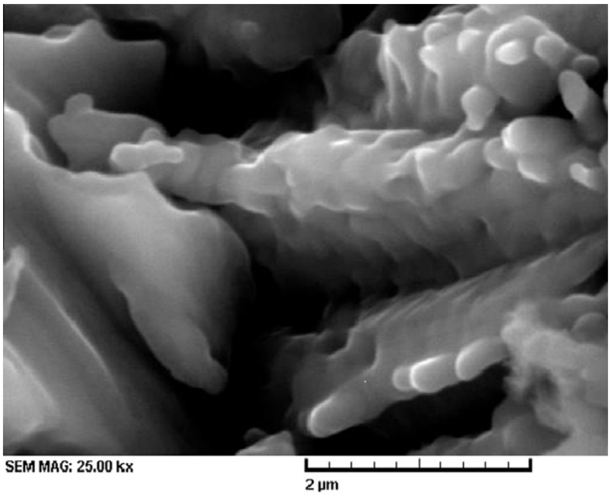

Fig. 8. SEM micrograph of silicide coating at high magnification.

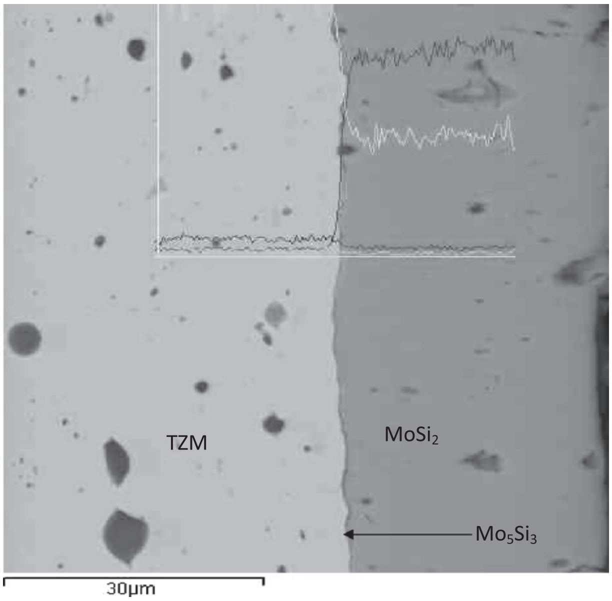

Fig. 9. SEM observation at the cross section of coating and substrate.

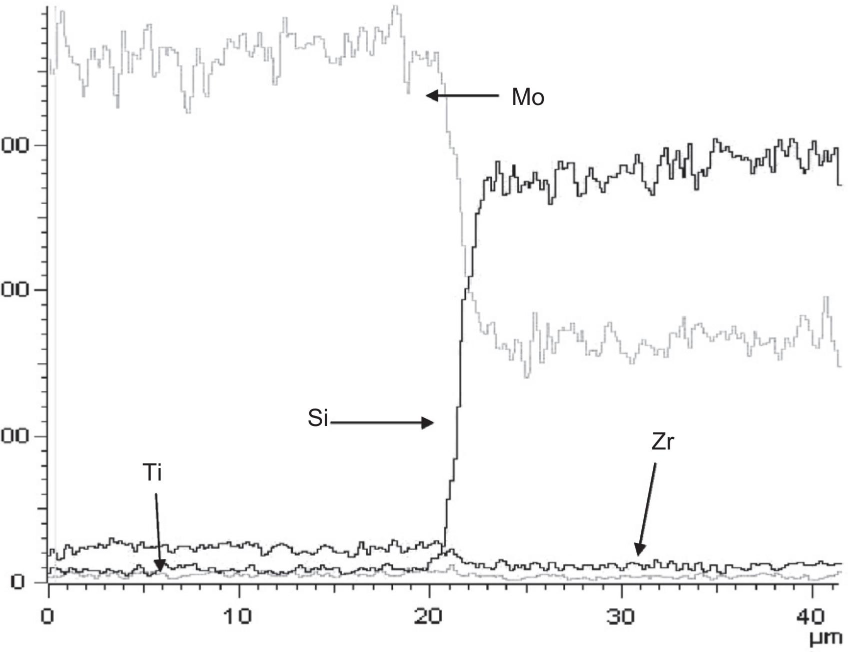

Fig. 10. EDX distribution profile of elements present in coated TZM alloy.

the substrate was very thin with approximately 1 µm thickness which was identified as Mo_5Si_3 and the thick outer layer of 100 µm was recognized as $MoSi_2$. Earlier, the XRD plot had revealed that there was no peak observed corresponding to Si in the coating other than $MoSi_2$. The absence of any Si particle from the pack in the coating of $MoSi_2$ obviously suggests the inward diffusion of Si which can be considered as the dominant mechanism of coating. The EDS concentration profile of Mo and Si in the coating and substrate as indicated in Fig. 10 revealed sudden reduction of Mo concentration adjacent to the substrate at the interface region of coating and substrate. The formation of Mo_5Si_3 layer on TZM substrate was the direct result of reduction in Mo concentration in this vicinity. Formation of this thin layer of Mo_5Si_3 was also verified by matching the intensity ratio of Mo and Si from the concentration profile of Mo and Si at Fig. 10 with the atomic ratio of Mo and Si in Mo_5Si_3 phase [4,10].

3.2.4. Evaluation of hardness and surface morphology

The hardness profile of the coated TZM alloy at the cross section was presented in Fig. 11. The micro-hardness distribution along the path of the coating was uniform with an average hardness value of 800 KHN. The hardness value however, shifted to 270 KHN as the diamond indentor reached the TZM alloy surface. The coating had shown comparatively higher hardness value than the uncoated alloy in view of its surface enhancement by the formation of hard coating of molybdenum di-silicide. The coating surface being hard was envisaged to have good resistance against wear.

3.2.5. Oxidation study of silicide coating on TZM alloy

The uncoated TZM alloy exhibited poor oxidation characteristics when heated under air as per the oxidation pattern as presented in Fig. 12. It was evident from the plot that the oxidation was sluggish at the initial stage and followed parabolic fashion

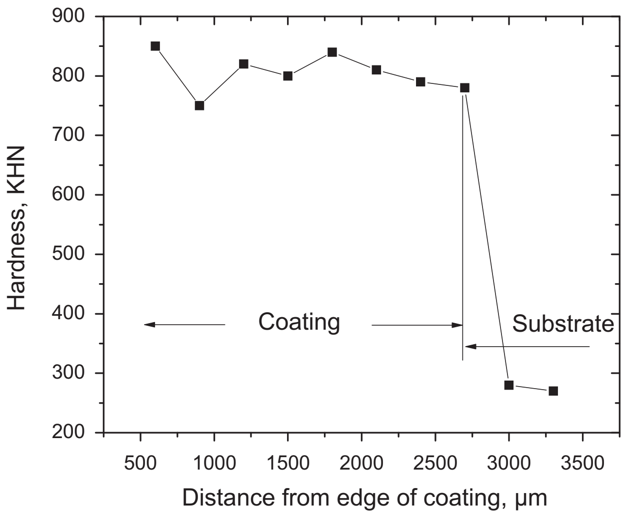

Fig. 11. Hardness profile on the surface of coated TZM alloy.

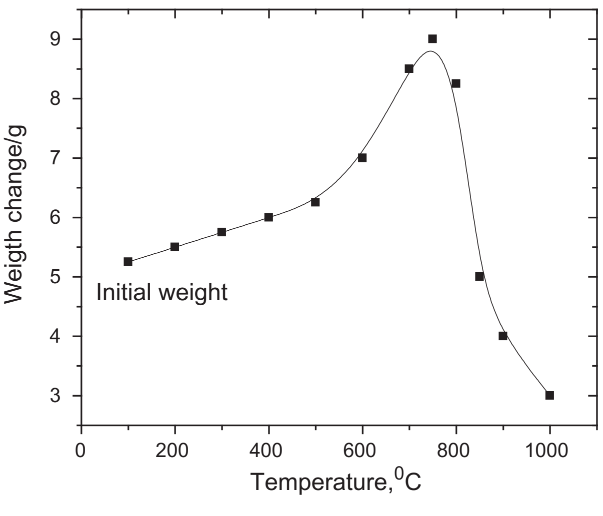

Fig. 12. Oxidation pattern of TZM alloy.

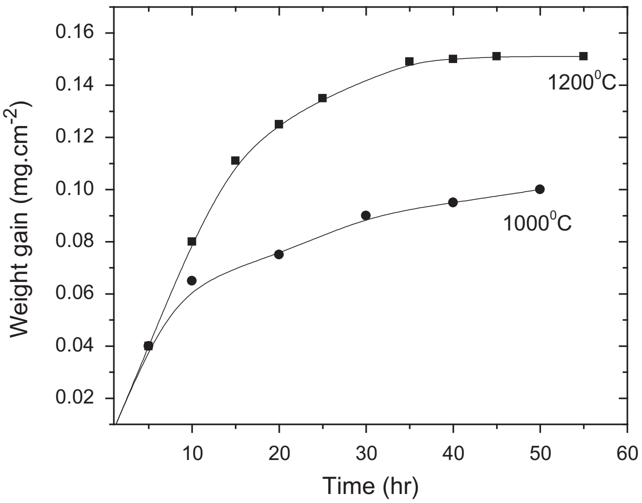

Fig. 13. Oxidation pattern of coated TZM alloy.

up to the temperature of 400 °C. The slow oxidation was due to the formation of the dark brown protective layer of non-volatile species, MoO_2 over the specimen surface. However, as the temperature was raised between 400 °C and 750 °C, there was a rapid oxidation due to the formation of highly volatile MoO_3 layers. Between temperatures 800 and 1000 °C, sharp loss in weight took place due to evaporation of the MoO_3. The cumulative weight gain was recorded to be in the range of 70–80 wt.% due to the formation of volatile oxide, MoO_3. However, there was neither any weight gain nor weight loss when the TZM specimen was heated under vacuum or argon.

The plot showing the oxidation pattern of the silicide coated TZM alloy under isothermal heating conditions was presented in Fig. 13. The excellent oxidation resistance exhibited by silicide coated TZM alloy in the temperature range of 1000–1200 °C was due to the formation of Si rich $MoSi_2$ phase as the matrix in the coating. $MoSi_2$ phase upon exposure to an oxidizing atmosphere, oxidizes to form a mixture of MoO_3 and SiO_2 species at low temperature (<800 °C) as per the chemical reaction (xi) and at high temperature (>800 °C), the oxidation is governed by the Eq. (xii) where silicide, Mo_5Si_3, forms between inner layer of $MoSi_2$ and outer layer of SiO_2. This outer layer of silicon di-oxide actually acts as a protective layer for the underlying substrate at high temperature [13].

$$2MoSi_2 + 7O_2 \rightarrow 2MoO_3 + 4SiO_2 \qquad \text{(xi)}$$

$$5MoSi_2 + 7O_2 \rightarrow Mo_5Si_3 + 7SiO_2 \qquad \text{(xii)}$$

The positive mass gain in the first 1–10 h heating cycle and the minimal mass gain between 10 and 50 h heating cycle as revealed by the plot, showed that the sample had produced a SiO_2 protective scale and that the underlying substrate was isolated from the atmosphere. It was observed at the end of the heating cycle, that no chipping or peeling of the coating took place from the coated surface.

4. Conclusions

Present investigation demonstrated the technical feasibility of developing silicide type of coating over TZM alloy substrate by pack cementation coating technique. A double layer coating structure was achieved within 12 h at 1000 °C under inert atmosphere. The thin inner layer of 1 μm thick adjacent to the substrate was identified as Mo_5Si_3 and the thick outer layer of 100 μm was identified as $MoSi_2$. The surface coating phase was confirmed to be $MoSi_2$ by XRD analysis. Inward diffusion of Si was the main mechanism of coating. The growth rate of coating was dominated by pack composition and time. Coating was uniformly formed all over the surfaces and adequately resistant to oxidation.

References

[1] G.R. Smolik, D.A. Petti, S.T. Schuetz, J. Nucl. Mater. 283–287 (2) (2000) 1458–1462.
[2] Z.D. Xiang, J.S. Burnell-Gray, P.K. Datta, J. Mater. Sci. 36 (2001) 5673–5682.
[3] S.P. Chakraborty, S. Banerjee, Kulwant Singh, I.G. Sharma, A.K. Grover, A.K. Suri, J. Mater. Process. Technol. 207 (1–3) (2008) 240–247.
[4] Sanjib Majumdar, Indrakumar Sharma, Indradev Samajdar, Parag Bhargavab, J. Electrochem. Soc. 155 (12) (2008) D734–D741.
[5] S. Majumdar, I.G. Sharma, A.K. Suri, Int. J. Refract. Metal Hard Mater. 26 (6) (2008) 549–554.
[6] Lai-rong Xiao, Zhi-gang Cai, D. Yi, Lei Ying, Hui-qun Liu, Dao-yuan Huang, Trans. Nonferrous Metal Soc. China 16 (1) (2006) 239–244.
[7] R. Sakidja, F. Rioult, J. Werner, J.H. Perepezko, Scr. Mater. 55 (2006) 903–906.
[8] W. Sheng, D. Liu, H.M. Wang, Surf. Coat. Technol. 202 (13) (2008) 2871–2877.
[9] S.R. Levine, R.M. Caves, J. Electrochem. Soc. 121 (1974) 1051–1064.
[10] Jin-Kook Yoon, Gyeung-Ho Kim, Ji-Young Byun, Jong-Kwon Lee, Ho-Sang Yoon, Kyung-Tae Hong, Surf. Coat. Technol. 172 (2003) 176–183.
[11] S.M. Tuominen, J.M. Dahl, J. Less Common Metals 81 (1981) 249–260.
[12] P.C. Tortorici, M.A. Dayananda, Metall. Mater. Trans. A 30 (1999) A545.
[13] Soo-Jin Park, Min-Kang Seo, Carbon 39 (2001) 1234.